Optimization of CSRR based RF sensor for detecting ethanol in petrol

Kunal Wadhwani
CVEST
International Institute of Information Technology (IIIT)
Hyderabad, India-500032
kunal.wadhwani@research.iiit.ac.in

Sheena Hussaini
MN Smart Radios, AD
Nokia of America Corporation
Dallas, TX, USA-75019
sheena.hussaini@nokia.com

Azeemuddin Syed
CVEST
International Institute of Information Technology (IIIT)
Hyderabad, India-500032
syed@iiit.ac.in

***Abstract*—This paper reports solvent based optimization of radio frequency (RF) sensors for detecting ethanol mixtures in petrol using complementary split ring resonators (CSRR). The optimization is carried out using binary particle swarm optimization (BPSO) in presence of mask by placing the sample under test (SUT) above the highly sensitive CSRR region. The motivation behind this work has been to detect miniscule changes of ethanol in the dielectric constant of the petrol. The RF sensors designed using BPSO enables faster convergence providing more efficient designs offering enhanced sensitivity at a normalized frequency of 2.66% and 1.81% when compared to 1.02% of conventional CSRR as presented in the simulation results.**

***Index Terms*—RF Sensor, CSRR, Optimization, Ethanol, BPSO, Petrol**

I. Introduction

The change in percentage of ethanol results in change in permittivity of the solution. E10 or 10% ethanol in gasoline (or petrol) causes substantial increase in emissions of acetaldehyde, with levels increasing by about 100–200% and in some cases by up to 700%. Acetaldehyde is hazardous compound known as carcinogen. Large increases in acetaldehyde emissions are also observed with E15 and E20. Ethanol is added for cost reduction of gasoline, leading to environmental problems which impacts air quality, sub-surface ground water contamination and also damages automobile engines in the long run. Hence, monitoring of the percentage amount of ethanol in gasoline plays a crucial role which requires sensitive methodology [1].

Optimization techniques in RF sensor design is the need of the hour. They have been used for antennas design [2], electromagnetic energy harvesters design [3] and microwave sensor design to attain desired properties for varied purposes. Heuristics like particle swarm optimization (PSO) [4], genetic algorithm [5] and differential evolution [6] have gained much more attention recently in the field of electromagnetics [7]. PSO is the most widely used algorithm in sensing, biology, communication and electronics [8]. It is preferred in comparison to other techniques due to its ease in implementation, excellent convergence accuracy, reduced dependency on initial conditions and reliability. The sensing region of the design is broken into multiple fragments called cells and the resulting design is called as cell patterned RF sensor. Each cell can be metalized or etched out. Thus, state of each cell can be represented using either 0 or 1. Therefore, binary version of PSO called binary particle swarm optimization (BPSO) [9], [10] to determine the best possible cell pattern.

RF sensors have been designed in the past using air as a reference [11], [12]. Such sensors suffer from low sensitivity when needed to detect minuscule changes of sample under test (SUT) in the dielectric constant of the solvent. In this work, the optimization of the RF sensor design is done both in presence of petrol (as a solvent) and air. The designs optimized in presence of solvent are called solvent based cell patterned designs. Whereas, the designs optimized in presence of air are called air based cell patterned designs. The sensitivity of the design is enhanced for detecting E10 ethanol in petrol. Solvent based optimization is preferred over air based optimization in order to achieve highly sensitive designs with lower convergence time of the algorithm. The dielectric constant of petrol and 10% ethanol in petrol solution are 2.16 and 2.38 respectively [13]. This methodology enables the design to be highly sensitive in the targeted range of dielectric constant of the solvent. These dielectric constants mentioned above are used for simulations of conventional CSRR [16]–[18], updated CSRR [19], air based cell patterned designs and solvent based cell patterned designs [20].

II. Optimization Methodology

More the normalized frequency (NF), more is the sensitivity of the RF design. NF is defined as

$$NF = \frac{\Delta f}{f_{petrol}} \tag{1}$$

where, f_{petrol} denotes the resonant frequency of the sensor when in pure petrol and Δf is given below

$$\Delta f = f_{ethanol-petrol} - f_{petrol} \tag{2}$$

where, $f_{ethanol-petrol}$ is the resonant frequency of the sensor when in ethanol-petrol blend. The algorithm is defined as a minima problem, so we define a mathematical parameter called cost function (CF) which is reciprocal of NF. The main goal

978-83-956020-3-0 ©2022 Warsaw University of Technology
MIKON-2022,Gdańsk, Poland

here is to achieve high sensitivity, hence reducing the CF in order to reach the minima corresponding to the convergence of the algorithm for providing desirable final design after optimization. The equation of the CF is given as follows

$$CF = \frac{1}{NF} = \frac{f_{petrol}}{\Delta f} \tag{3}$$

Initial design (in this case, Updated CSRR) will be used as a reference design for all the designs generated mid-way during the optimization procedure and for the final design obtained after optimization ends. The initial design will have a CF value which will relate to its sensitivity towards sensing certain dielectric constant change. Each combination of the cells result in a different design structure offering a distinguishing CF value. A group of particles is equipped for exploring the k-dimensional search space widely that are called the swarm size. The swarm size is set to 30, which is optimum for PSO based heuristic, as reported in [14]. The swarm of particles are initialized with the particle position (X) of the initial design used by the equation of the PSO given below

$$V_n^{t+1} = wV_n^t + a_1 r_1 (P_n^t - X_n^t) + a_2 r_2 (G^t - X_n^t) \tag{4}$$

where V_n is the velocity of the n^{th} particle, X_n is the position of the n^{th} particle, t denotes the iteration number, w is called the inertia weight, P_n is the personal best solution of the n^{th} particle, G is the global best solution of the whole swarm, a_1 is personal acceleration coefficient contributing in accelerating the movement of particle towards best experienced solution by the particle and a_2 is social acceleration coefficient contributing in accelerating the movement of particle towards the best experienced solution by the entire swarm. Here, V, X, P, and G are k-dimensional vectors. The values of w, a_1 and a_2 are 1, 2 and 2 respectively as stated in [15] for better convergence.

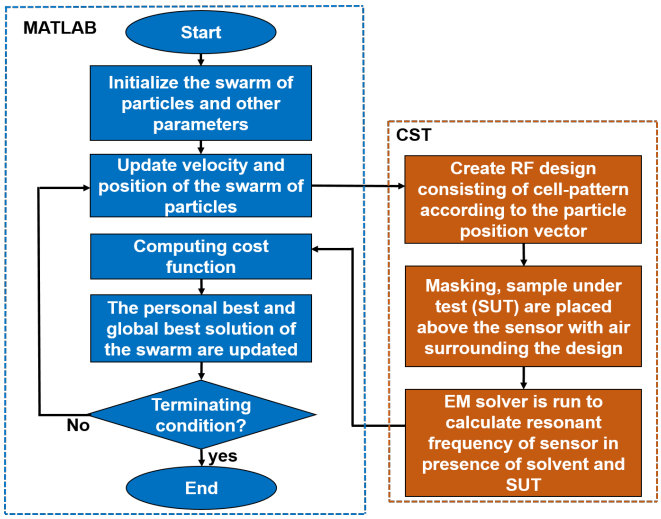

Fig. 1. Flow chart of the optimization procedure.

The initial velocity vector V_n is varied randomly from 0 to L, where L denotes the particle's dynamic range in every dimension to restrict the particle's motion outside the problem's search space. The initial design is assumed to be the personal best and global best solution initially until we achieve a new design that is more sensitive through several iterations. Then, velocity vector and position vector are updated using Eqn (4) respectively. The sigmoid function is used to convert the continuous particle velocity into discrete or binary particle position using the equation given as follows

$$S(V_n^{t+1}) = \frac{1}{1 + exp(-V_n^{t+1})} \tag{5}$$

The position of the n^{th} particle at the $t+2$ iteration is given by

$$X_n^{t+2} = \begin{cases} 1, & S(V_n^{t+1}) > r \\ 0, & S(V_n^{t+1}) \leq r \end{cases} \tag{6}$$

where r is a random number uniformly distributed between 0 and 1. Then, using Eqn (6) the particle position becomes a strings of 0s and 1s. The controlling tool is MATLAB which consists of the BPSO algorithm. It controls the electromagnetic simulations done by CST Microwave Studio. The simulations are performed in presence of mask and sample surrounded by the air box. Air box is used in the simulation in order to match the physical ambient conditions in the experimental setup. After running simulations, the values of $f_{solution}$ and $f_{solvent}$ are transferred from CST to MATLAB for calculation of Δf and CF. The concept of personal best and global best can be related to concept of local minima and a global minima in the algorithms. Then, personal best and global best solution are updated for the current iteration. As the iterations proceed, the position and velocity of each swarm particle of the population are modified to move vectorially towards the personal best solution and the global best solution in accordance to Eqn (4). The whole optimization procedure is concisely depicted in Fig. 1. Considering the algorithm's convergence by few test runs and observing acceptable computational time, we take the maximum number of iterations as 50. The algorithm is terminated at the end of 50 iterations. The variation of cost function with respect to the number of iterations is seen in Fig. 2.

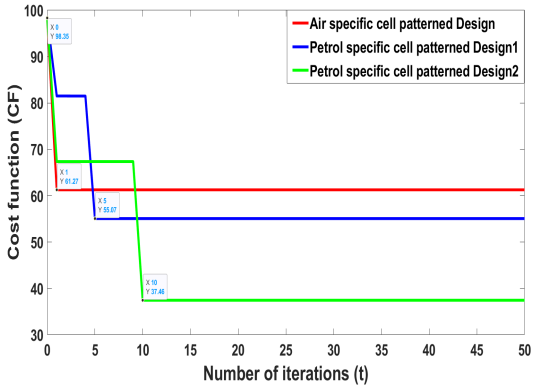

Fig. 2. Cost function vs Number of iteration

III. Simulation

All the sensors are simulated using a FR-4 substrate of thickness 1.6 mm and dielectric constant of 4.3 with copper as the conductor of thickness 0.035 mm on both sides. The designs were optimized using BPSO in the frequency range of 0-5 GHz. Later, only the frequency of interest i.e. the resonant frequency of the sensor in presence of petrol and ethanol-petrol blend is shown in the simulation results.

Fig. 3 shows the back view consisting of microstrip line in conventional CSRR, updated CSRR, air based cell patterned designs and solvent based cell patterned designs.

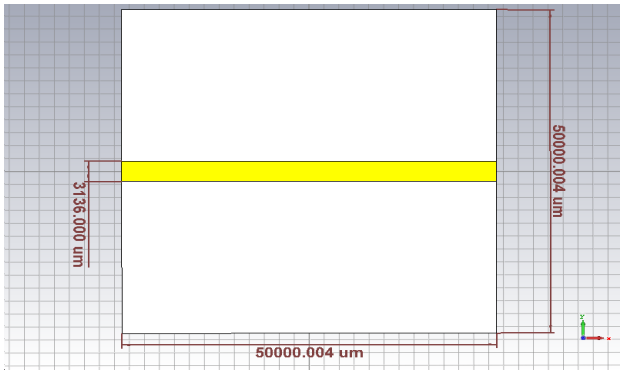

Fig. 3. Back view of all the sensors (conventional CSRR, updated CSRR, cell patterned CSRR).

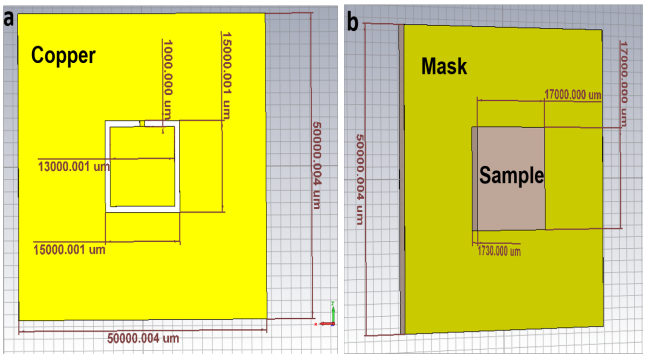

Fig. 4. (a). Front view of conventional CSRR based RF sensor with dimensions in μm.. (b). Front view of all sensors with SUT above the sensing region with dimensions in μm..

Fig. 4 (a) shows the front view of conventional CSRR of size 50×50 mm^2 with all dimensions mentioned in μm. Fig. 4 (b) shows front view of all sensors described in this section. It depicts the mask layer thickness 0.035 mm placed above the copper and the sample of size 17×17 mm^2 placed above the mask on the sensing region of the sensor. The thickness of sample is decided as 1.73 mm in order to make the volume equal to 500 μl. The cell size is selected as 1 mm as it is the minimum feature size for PCB fabrication with high accuracy. The sensing region is of 17×17 mm^2 size. The S-parameter simulation response of conventional CSRR is depicted in Fig. 5 for testing ethanol-petrol. The sensor resonates at 1.47 GHz for petrol and at 1.455 GHz for 10% ethanol solution.

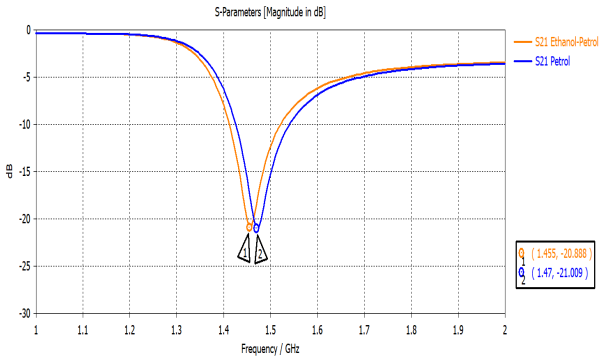

Fig. 5. Magnitude of S_{21} (dB) vs frequency (GHz) for Conventional CSRR for ethanol-petrol.

Fig. 6 shows the front view of updated CSRR of size 50×50 mm^2 with all dimensions mentioned in μm. The S-parameter simulation response for this design is depicted in Fig. 7 for sensing ethanol-petrol. The sensor resonates at 1.485 GHz for petrol and at 1.47 GHz for 10% ethanol solution.

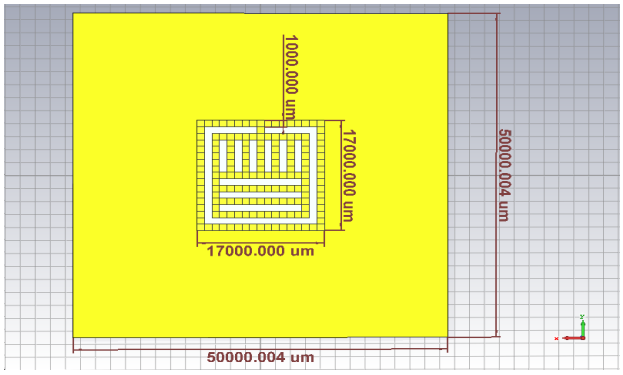

Fig. 6. Front view of Updated CSRR based RF sensor with dimensions in μm.

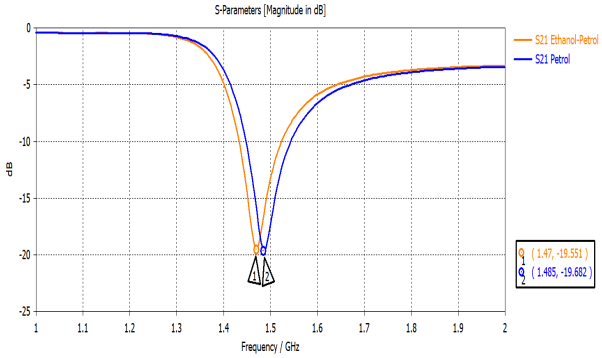

Fig. 7. Magnitude of S_{21} (dB) vs frequency (GHz) for Updated CSRR for ethanol-petrol.

Fig. 8 shows the front view of air based cell patterned CSRR of size 50×50 mm^2 with all dimensions mentioned in μm. The S-parameter simulation response for this design is depicted in

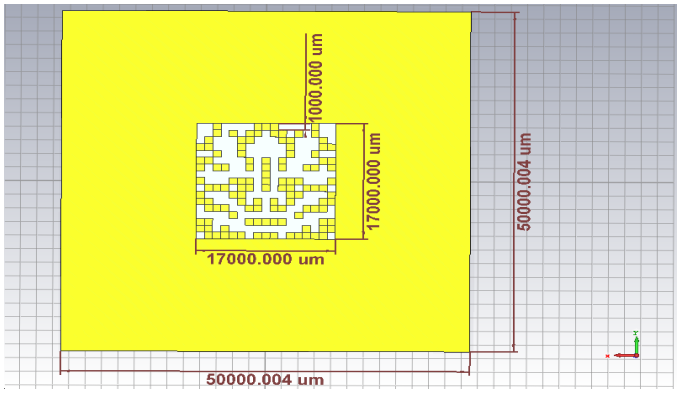

Fig. 8. Front view of Air based cell patterned CSRR based RF sensor for ethanol-petrol.

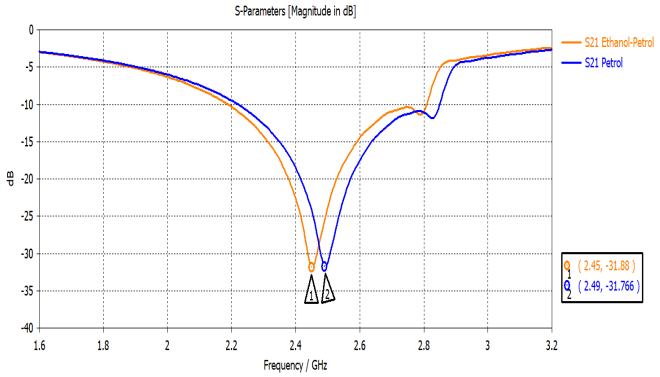

Fig. 9. Magnitude of S_{21} (dB) vs frequency (GHz) for Air based cell patterned for ethanol-petrol.

Fig. 9 for sensing ethanol-petrol. The sensor resonates at 2.49 GHz for petrol and at 2.45 GHz for 10% ethanol solution.

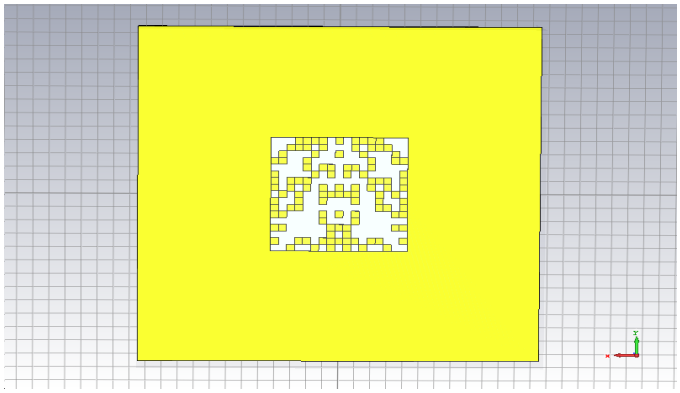

Fig. 10. Front view of Solvent based cell patterned Design1 for ethanol-petrol.

Fig. 10 shows the front view of Solvent based cell patterned Design1 of size 50×50 mm^2. The S-parameter simulation response for this sensor is depicted in Fig. 11 for sensing ethanol-petrol. The sensor resonates at 3.785 GHz for petrol and at 3.855 GHz for 10% ethanol solution.

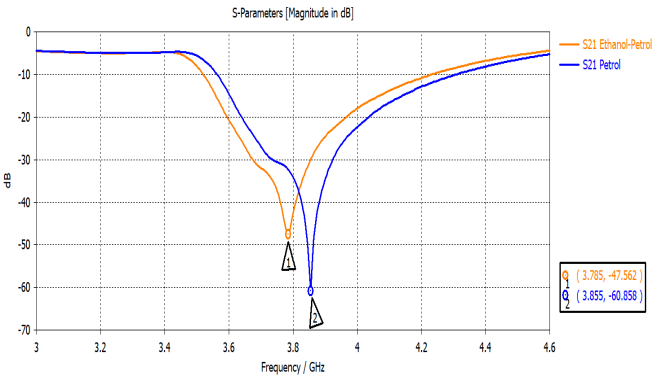

Fig. 11. Magnitude of S_{21} (dB) vs frequency (GHz) for Solvent based cell patterned Design1 for ethanol-petrol.

Fig. 12 shows the front view of Solvent based cell patterned Design2 of size 50×50 mm^2. The S-parameter simulation response for this sensor is depicted in Fig. 13 for sensing ethanol-petrol. The sensor resonates at 4.812 GHz for petrol and at 4.944 GHz for 10% ethanol solution.

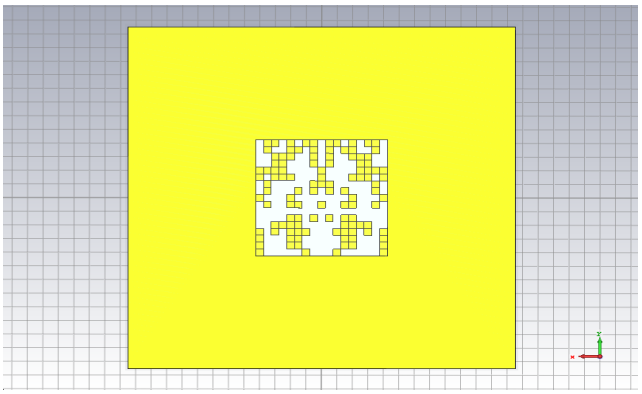

Fig. 12. Front view of Solvent based cell patterned Design2 for ethanol-petrol.

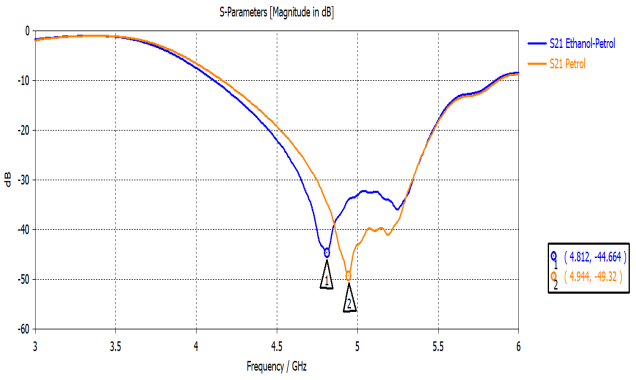

Fig. 13. Magnitude of S_{21} (dB) vs frequency (GHz) for Solvent based cell patterned Design2 for ethanol-petrol.

Table I shows the comparison of above discussed designs for sensing of ethanol-petrol in terms of $f_{solvent}$, Δf and NF.

TABLE I
COMPARISON OF VARIOUS DESIGNS

Design Type	f_{petrol}	Δf	NF
Conventional CSRR	1.47 GHz	0.015 GHz	0.0102
Updated CSRR (before optimization)	1.485 GHz	0.015 GHz	0.0101
Air specific cell patterned Design (after air based optimization)	2.45 GHz	0.04 GHz	0.01632
Petrol specific cell patterned Design1 (after petrol based optimization)	3.855 GHz	0.07 GHz	0.01815
Petrol specific cell patterned Design2 (after petrol based optimization)	4.944 GHz	0.132 GHz	0.02669

CONCLUSION

This paper presents the importance of solvent based optimization for RF sensors with maximized sensitivity using BPSO. The simulation results clearly depict that high efficiency and sensitivity enhancement has been achieved for RF sensors for detecting ethanol in ethanol-petrol mixtures using cell-patterned CSRR designs. Moreover, the presented technique is highly desired and can also be applied for detection of any SUT in solvent.

REFERENCES

[1] R. K. Niven, "Ethanol in gasoline: Environmental impacts and sustainability review article," Renewable and sustainable energy reviews, vol. 9, no. 6, pp. 53.

[2] A. Modiri and K. Kiasaleh, "Efficient design of microstrip antennas for sdr applications using modified pso algorithm," IEEE Transactions on Magnetics, vol. 47, no. 5, pp. 1278–1281, 2011.

[3] B. Ghaderi, V. Nayyeri, M. Soleimani, and O. M. Ramahi, "Pixelated metasurface for dual-band and multi-polarization electromagnetic energy harvesting," Scientific reports, vol. 8, no. 1, pp. 1– 12, 2018.

[4] N. Jin and Y. Rahmat-Samii, "Advances in particle swarm optimization for antenna designs: Real-number, binary, single-objective and multiobjective implementations," IEEE transactions on antennas and propagation, vol. 55, no. 3, pp. 556–567, 2007.

[5] M. Lamsalli, A. El Hamichi, M. Boussouis, N. A. Touhami, and T. Elhamadi, "Genetic algorithm optimization for microstrip patch antenna miniaturization," Progress In Electromagnetics Research Letters, vol. 60, pp. 113–120, 2016.

[6] I. M. Danjuma, M. O. Akinsolu, C. H. See, R. A. Abd-Alhameed, and B. Liu, "Design and optimization of a slotted monopole antenna for ultra-wide band body centric imaging applications," IEEE Journal of Electromagnetics, RF and Microwaves in Medicine and Biology, vol. 4, no. 2, pp. 140–147, 2020.

[7] S. H. Yeung, W. S. Chan, K. T. Ng, and K. F. Man, "Computational optimization algorithms for antennas and rf/microwave circuit designs: An overview," IEEE Transactions on Industrial Informatics, vol. 8, no. 2, pp. 216–227, 2012.

[8] Y. Zhang, S. Wang, and G. Ji, "A comprehensive survey on particle swarm optimization algorithm and its applications," Mathematical problems in engineering, vol. 2015, 2015.

[9] J. Kennedy and R. C. Eberhart, "A discrete binary version of the particle swarm algorithm," 1997 IEEE International Conference on Systems, Man, and Cybernetics. Computational Cybernetics and Simulation, 1997, pp. 4104-4108 vol.5.

[10] N. Jin and Y. Rahmat-Samii, "Advances in Particle Swarm Optimization for Antenna Designs: Real-Number, Binary, Single-Objective and Multiobjective Implementations," in IEEE Transactions on Antennas and Propagation, vol. 55, no. 3, pp. 556-567, March 2007.

[11] M. Saadat-Safa, V. Nayyeri, A. Ghadimi, M. Soleimani, and O. M. Ramahi, "A pixelated microwave near-field sensor for precise characterization of dielectric materials," Scientific reports, vol. 9, no. 1, pp. 1–12, 2019.

[12] K. Wadhwani, S. Hussaini and A. Syed, "Real-time Quantitative Analysis of L-Lysine Based on Radio Frequency Sensing," 2020 IEEE MTT-S International Microwave Biomedical Conference (IMBioC), 2020, pp. 1-3.

[13] A. Kunte and S. Kulkarni, "Experimental investigation of complex permittivity determination of ethanol content in gasoline," in 2008 International Conference on Recent Advances in Microwave Theory and Applications, IEEE, 2008, pp. 171–174.

[14] X. Zhang, D. Lu, X. Zhang, and Y. Wang, "Antenna array design by a contraction adaptive particle swarm optimization algorithm," EURASIP Journal on Wireless Communications and Networking, vol. 2019, no. 1, pp. 1–7, 2019.

[15] J. Dong, Q. Li, and L. Deng, "Design of fragment-type antenna structure using an improved bpso," IEEE Transactions on Antennas and Propagation, vol. 66, no. 2, pp. 564–571, 2017.

[16] M. S. Boybay and O. M. Ramahi, "Material Characterization Using Complementary Split-Ring Resonators," in IEEE Transactions on Instrumentation and Measurement, vol. 61, no. 11, pp. 3039-3046, Nov. 2012.

[17] M. A. H. Ansari, A. K. Jha and M. J. Akhtar, "Design and Application of the CSRR-Based Planar Sensor for Noninvasive Measurement of Complex Permittivity," in IEEE Sensors Journal, vol. 15, no. 12, pp. 7181-7189, Dec. 2015.

[18] A. Ebrahimi, W. Withayachumnankul, S. Al-Sarawi and D. Abbott, "High-Sensitivity Metamaterial-Inspired Sensor for Microfluidic Dielectric Characterization," in IEEE Sensors Journal, vol. 14, no. 5, pp. 1345-1351, May 2014.

[19] A. M. Albishi and O. M. Ramahi, "Microwaves-Based High Sensitivity Sensors for Crack Detection in Metallic Materials," in IEEE Transactions on Microwave Theory and Techniques, vol. 65, no. 5, pp. 1864-1872, May 2017.

[20] K. Wadhwani, S. Hussaini, A. Mazumder and A. Syed, "Solvent-Based Optimization of CSRR and IDC RF Bio-Sensors," in IEEE Sensors Journal, vol. 22, no. 6, pp. 5651-5661, 2022.